Caenorhabditis elegans Aurora A kinase is required for the formation of spindle microtubules in female meiosis

Eisuke Sumiyoshi, Yuma Fukata, Satoshi Namai, and Asako Sugimoto
Laboratory of Developmental Dynamics, Graduate School of Life Sciences, Tohoku University, Sendai 980-8577, Japan

ABSTRACT **In many animals, female meiotic spindles are assembled in the absence of centrosomes, the major microtubule (MT)-organizing centers. How MTs are formed and organized into meiotic spindles is poorly understood. Here we report that, in *Caenorhabditis elegans*, Aurora A kinase/AIR-1 is required for the formation of spindle microtubules during female meiosis. When AIR-1 was depleted or its kinase activity was inhibited in *C. elegans* oocytes, although MTs were formed around chromosomes at germinal vesicle breakdown (GVBD), they were decreased during meiotic prometaphase and failed to form a bipolar spindle, and chromosomes were not separated into two masses. Whereas AIR-1 protein was detected on and around meiotic spindles, its kinase-active form was concentrated on chromosomes at prometaphase and on interchromosomal MTs during late anaphase and telophase. We also found that AIR-1 is involved in the assembly of short, dynamic MTs in the meiotic cytoplasm, and these short MTs were actively incorporated into meiotic spindles. Collectively our results suggest that, after GVBD, the kinase activity of AIR-1 is continuously required for the assembly and/or stabilization of female meiotic spindle MTs.**

Monitoring Editor
Susan Strome
University of California, Santa Cruz

Received: May 1, 2015
Revised: Sep 1, 2015
Accepted: Sep 9, 2015

INTRODUCTION

In female meiosis, two rounds of highly asymmetric meiotic divisions produce a single oocyte that inherits the majority of cytoplasm, with excluded polar bodies. In contrast to mitotic spindles, which consist of microtubules (MTs) formed mainly at centrosomes, female meiotic spindles in many animals are assembled in the absence of centrosomes, which are eliminated during oogenesis (Sawada and Schatten, 1988; Gard, 1992; Schatten, 1994).

Centrosome-independent MT assembly in meiosis has been characterized in several model systems. In extracts of *Xenopus* oocytes arrested at G2/M in meiotic prophase I, condensed chromosomes can promote MT assembly (Heald *et al.*, 1996; Khodjakov *et al.*, 2000) in a manner dependent on the small GTPase Ran (Carazo-Salas *et al.*, 1999; Gruss *et al.*, 2001; Nachury *et al.*, 2001). In mouse oocytes, >80 microtubule-organizing centers (MTOCs) are formed during meiotic prophase, which then cluster and increase MT mass in a RanGTP-dependent manner (Schuh and Ellenberg, 2007). However, it was also reported that Ran might be dispensable for the formation of the female meiosis I spindle in mice and *Xenopus* (Dumont et al., 2007), implying that multiple MT assembly pathways may contribute to the formation of female meiotic spindles in vertebrates.

As in vertebrates, female meiotic spindles of the nematode *Caenorhabditis elegans* are formed in the absence of centrosomes (Figure 1; Albertson and Thomson, 1993; McNally *et al.*, 2006; Dumont *et al.*, 2010). Whereas the γ-tubulin complex, a conserved MT nucleator, is essential for assembly of normal female meiotic spindles in *Drosophila* and mice (Tavosanis *et al.*, 1997; Barrett and Albertini, 2007; Ma *et al.*, 2010), previous studies indicated that this complex is dispensable for the formation of meiotic spindles in *C. elegans* (Bobinnec *et al.*, 2000; McNally *et al.*, 2006). It is unknown how MTs composing female meiotic spindles are assembled in *C. elegans* embryos.

Aurora A is a conserved mitotic kinase required for centrosome maturation and spindle assembly in many organisms, including *C. elegans* (Glover *et al.*, 1995; Schumacher *et al.*, 1998a; Hannak *et al.*, 2001; Barros *et al.*, 2005; Tsai and Zheng, 2005; Lioutas and Vernos, 2013; Reboutier *et al.*, 2013). In mouse oocytes, depletion

This article was published online ahead of print in MBoC in Press (http://www.molbiolcell.org/cgi/doi/10.1091/mbc.E15-05-0258) on September 16, 2015.

Address correspondence to: Asako Sugimoto (asugimoto@m.tohoku.ac.jp).

Abbreviations used: GVBD, germinal vesicle breakdown; MT, microtubule; MTOC, microtubule-organizing center.

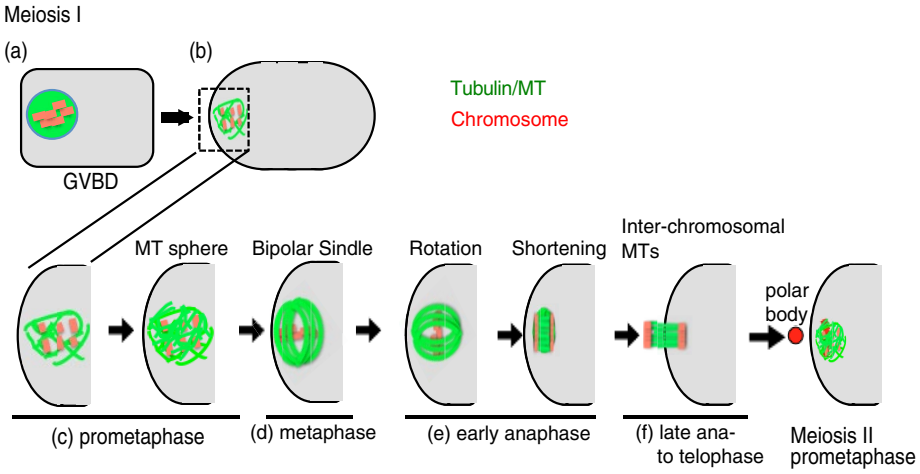

FIGURE 1: Formation of a female meiotic spindle in *C. elegans* from GVBD at meiosis I to the beginning of meiosis II. MTs and chromosomes are indicated by green and red, respectively.

of Aurora A causes mislocalization of MTOCs and formation of aberrant female meiotic spindles (Ding *et al.*, 2011). Previously we reported that, during mitosis in *C. elegans* early embryos, the kinase-inactive form of Aurora A/AIR-1 is required for the assembly or stabilization of γ-tubulin–independent MTs (Motegi *et al.*, 2006; Toya *et al.*, 2011). However, it has not been investigated whether AIR-1 is involved in the formation of female meiotic spindles.

In this study, we analyzed the roles of AIR-1 in *C. elegans* female meiotic spindle formation. We found that, whereas the kinase activity of AIR-1 is likely dispensable for the initial MT assembly at germinal vesicle breakdown (GVBD), it is essential for the formation and/or maintenance of spindle MTs throughout meiosis after GVBD.

RESULT AND DISCUSSION

AIR-1 is required for stabilization of MTs around chromosomes during prometaphase/metaphase of female meiosis

To examine the functional requirement of AIR-1 in *C. elegans* female meiosis, we observed MT behaviors in live *air-1(RNAi)* meiotic embryos expressing green fluorescent protein (GFP)::β-tubulin and mCherry::Histone.

In control RNA interference (RNAi) embryos (18 of 18), formation of the female meiotic spindle occurred as previously described (Figures 1 and 2Aa and Supplemental Video S1a; Albertson and Thomson, 1993; Yang *et al.*, 2003; McNally *et al.*, 2006; Dumont *et al.*, 2010). At the onset of GVBD during oocyte maturation, β-tubulin signals accumulated, and MTs were formed in the oocyte nucleus located near the distal cortex (Figure 2Aa, 120 s). The MTs and condensed chromosomes were then assembled into a spherical structure (Figure 2Aa, 420 s). This MT sphere migrated toward the cortex and became bipolar at metaphase (Figure 2Aa, 720 s). At anaphase, the bipolar spindle rotated 90° and shortened along its bipolar axis (Figure 2Aa, 1200 s). As the bipolar spindle MTs gradually decreased, interchromosomal MTs were formed between segregating homologous chromosomes (Figure 2Aa, 1440 s), followed by polar body exclusion. The second meiotic spindles were formed in a similar manner.

In all *air-1(RNAi)* meiotic embryos (13 of 13), MTs were formed in the oocyte nucleus at early prometaphase as in the control embryos (Figure 2Ab, 120 s), whose amount was equivalent to that of the control (median of relative fluorescent intensity of GFP:: β-tubulin at 120 s after GVBD; 2.39 arbitrary units (a.u.) in the control ($n = 6$) and 2.59 a.u. in *air-1(RNAi)* ($n = 5$; $p > 0.1$; Figure 2Ba). These MTs formed sphere-like structures around chromosomes as they migrated toward the cortex (Figure 2Ab, 420 s). However, the MT spheres shrunk without forming bipolar spindles, and chromosomes were never aligned (Figure 2Ab, 420–780 s, and Supplemental Video S1b). The MTs composing the spheres were significantly decreased by the time corresponding to metaphase to early anaphase in the control embryos (at 720 s after GVBD; 2.54 a.u. in the control [$n = 6$] and 2.12 a.u. in *air-1(RNAi)* [$n = 5$], $p < 0.01$; Figure 2B). This shrinkage of MT spheres in the *air-1(RNAi)* embryos occurred substantially earlier than the spindle shortening at anaphase in the control embryos, and eventually MTs became nearly undetectable (Figure 2Ab, 780 s). Subsequently, MTs—likely to correspond to the meiosis II spindle MTs—were often reassembled around chromosomes to form sphere-like structures, which also shrunk and disappeared without forming bipolar spindles (unpublished data). These observations indicate that, in contrast to early mitosis, in which AIR-1 is essential for the assembly of chromatin-dependent MTs (Toya *et al.*, 2011), the major role of AIR-1 in female meiosis is to maintain MTs formed around chromosomes but not the initial MT assembly.

Previous studies reported that RNAi depletion of γ-tubulin (TBG-1) in *C. elegans* embryos did not inhibit meiotic spindle assembly (Bobinnec *et al.*, 2000; McNally *et al.*, 2006), which was confirmed by our observation using mCherry::TBG-1–expressing embryos. In the *tbg-1(RNAi)* embryos, whereas the mCherry::TBG-1 signal was undetectable and mitotic spindle formation was severely inhibited (Supplemental Figure S1), meiotic spindle formation was unaffected (5 of 5 embryos; Figure 2Ac and Supplemental Video S1c). The fluorescence intensities of GFP::β-tubulin in the meiotic spindle regions in *tbg-1(RNAi)* embryos were not significantly reduced at either 120 or 720 s after GVBD ($n = 5$, $p > 0.05$; Figure 2B). To examine whether γ-tubulin contributes to the assembly of meiotic nuclear MTs in the absence of AIR-1, we observed the female meiosis in *air-1(RNAi);tbg-1(RNAi)* embryos. In these embryos, although mitotic spindle MTs were barely formed (Supplemental Figure S1A), the amount of meiotic MTs around chromosomes was equivalent to that of *air-1(RNAi)* embryos (Figure 2, Ad and B, and Supplemental Video S1d). These results suggest that formation of MTs in meiotic nuclei requires neither γ-tubulin nor AIR-1 but that a previously unknown MT formation pathway is likely involved. (Because of the technical limitation of RNAi experiments, we cannot exclude the possibility that trace amounts of γ-tubulin and AIR-1 that are insufficient to form mitotic MTs might be sufficient for meiotic MT assembly.)

To analyze further which process of meiotic spindle formation is defective in *air-1(RNAi)* embryos, we observed the localization of ASPM-1, the orthologue of *Drosophila* Abnormal Spindle (Asp; Riparbelli *et al.*, 2002; van der Voet *et al.*, 2009), which localizes to poles of meiotic spindles and is redundantly required for establishing bipolarity of meiotic spindles (Connolly *et al.*, 2014). In control embryos, GFP::ASPM-1 at prometaphase was detected as multiple foci on MTs around chromosomes (Figure 2Ca), which then gradually gathered at two spindle poles at metaphase and early anaphase (5 of 5 embryos; Figure 2Cb). In *air-1(RNAi)* meiotic embryos during

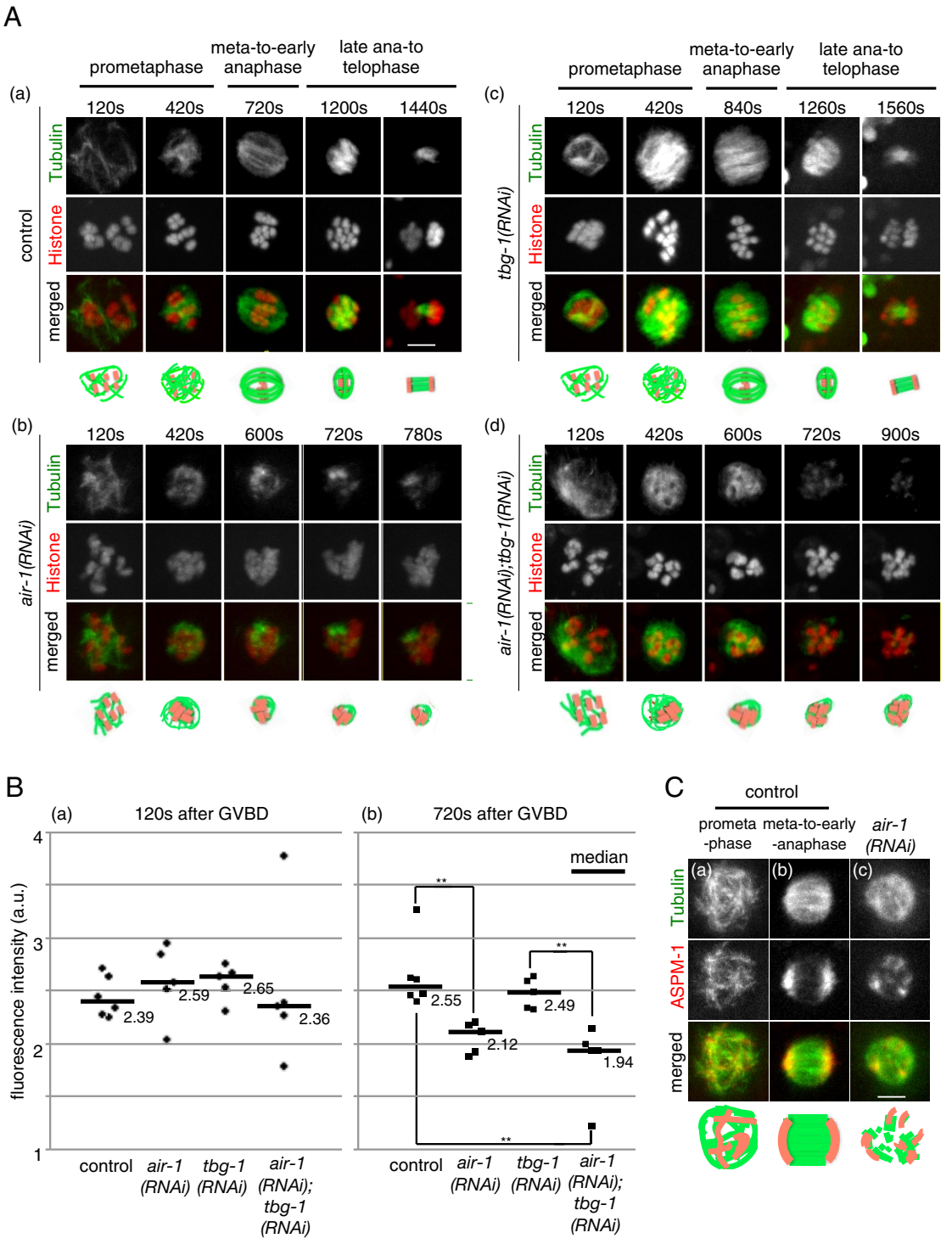

FIGURE 2: AIR-1 is required for the formation of female meiotic spindles. (A) In utero time-series images of female meiotic spindles visualized by GFP::β-tubulin (green) and mCherry::Histone (red). (a) Control, (b) *air-1(RNAi)*, (c) *tbg-1(RNAi)*, and (d) *air-1(RNAi);tbg-1(RNAi)* embryos. Frames were taken every 60 s, and representative images are shown. The time (in seconds) relative to GVBD is indicated. Bar, 5 μm. (B) Quantification of meiotic spindle MTs. Each dot represents the relative fluorescence intensity of GFP::β–tubulin in the meiotic spindle regions normalized with the fluorescence intensity of mCherry::Histone ($n = 5$). (a) Prometaphase (120 s after GVBD). (b) Metaphase to early anaphase (720 s after GVBD). Pairs with significant difference, $^{**}p < 0.01$. (C) In utero live images of meiotic spindle MTs visualized with mCherry::β-tubulin (green) and GFP::ASPM-1 (red). (a) MT sphere at prometaphase in a control embryo. (b) Bipolar spindle at early anaphase in a control embryo. (c) MT sphere in an *air-1(RNAi)* embryo. Bar, 5 μm.

the shrinkage of MT spheres, GFP::ASPM-1 was detected as more than two foci (5 of 5 embryos) (Figure 2Cc), indicating that the MT spheres failed to establish bipolarity.

In mitosis of *C. elegans* early embryos, the kinase activity of AIR-1 is required for centrosome maturation but is dispensable for the formation/maintenance of MTs assembled around chromosomes

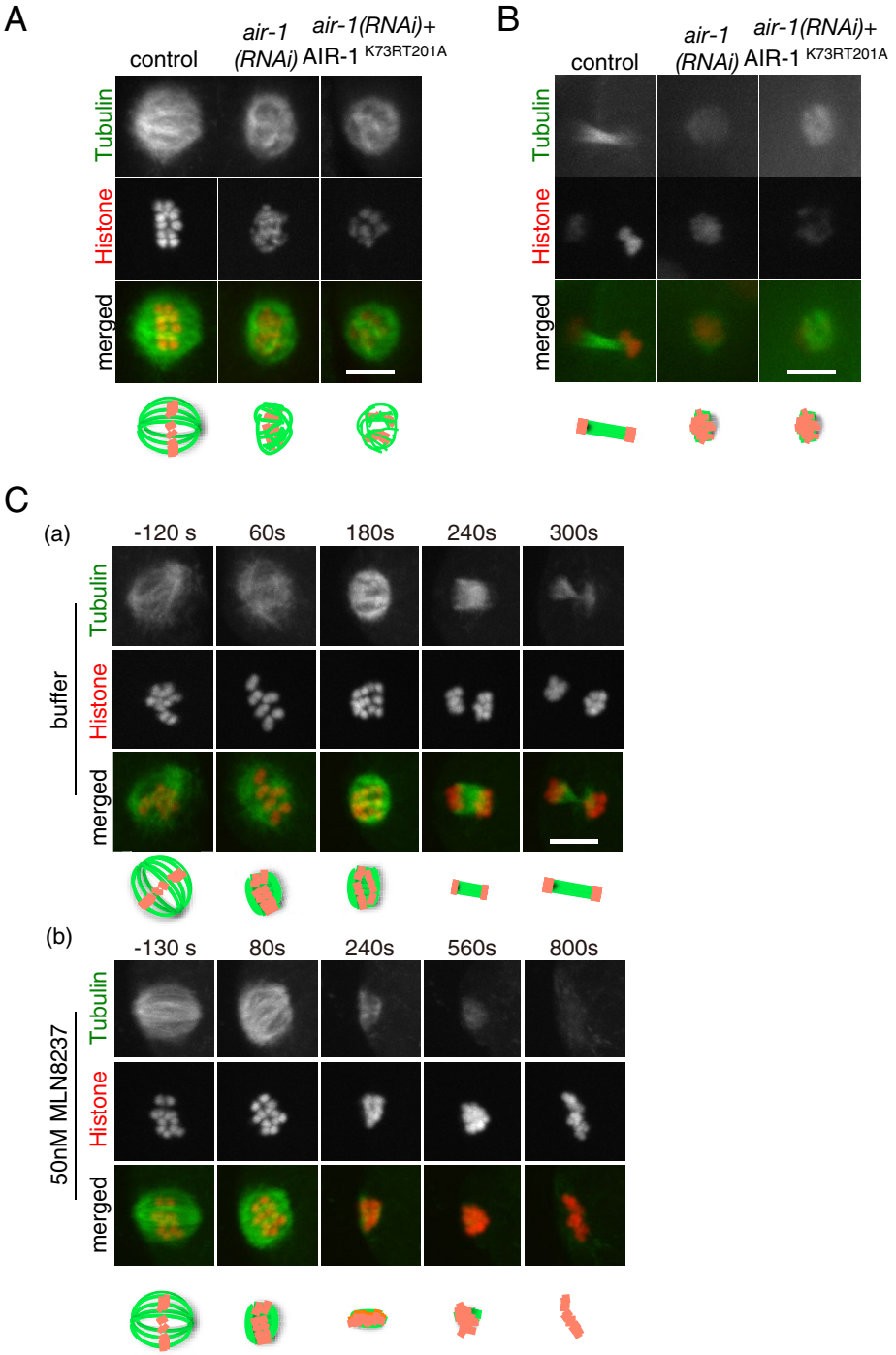

FIGURE 3: Kinase activity of AIR-1 is continuously required for the formation/maintenance of MTs after bipolar spindle establishment (A) Ex vivo live images of meiotic spindles visualized by GFP::β-tubulin (green) and mCherry::Histone (red). Control embryo at early anaphase, *air-1(RNAi)* embryo, and *air-1(RNAi)* embryo expressing mCherry::AIR-1$^{K73R\ T201A}$ (kinase-inactive form; not visible with this image contrast) are shown. Bar, 5 μm. (B) In utero live images of meiotic MTs visualized by GFP::β-tubulin (green) and mCherry::Histone (red). Interchromosomal MTs of a control embryo at late anaphase, *air-1(RNAi)* embryo, and *air-1(RNAi)* embryo expressing the kinase-inactive form mCherry::AIR-1$^{K73R\ T201A}$ (kinase-inactive form; not visible with this image contrast) at equivalent stages are shown. Bar, 5 μm. (C) Ex vivo time-series images of female meiotic spindles visualized by GFP::β-tubulin (green) and mCherry::Histone (red). (a) Control (buffer only) and (b) treatment with 50 nM MLN8237 (Aurora A kinase inhibitor). Buffer or MLN8237 was administered at 0 s. Frames were taken every 60 (a) and 80 (b) s, and representative images are shown. Bar, 5 μm.

(Hannak *et al.*, 2001; Toya *et al.*, 2011). Therefore we examined whether the assembly of meiotic spindles requires the kinase activity of AIR-1, using the embryos expressing wild-type GFP::AIR-1 or a kinase-inactive form of mCherry::AIR-1 (AIR-1^{K73RT201A}) from RNAi-resistant transgenes (Figure 3A and Supplemental Figure S2). In both transgenic strains, the protein levels of transgenic AIR-1 or AIR-1^{K73RT201A} were approximately half of the endogenous AIR-1 (Supplemental Figure S2A). Under the condition that the endogenous AIR-1 was depleted by RNAi, the wild-type GFP::AIR-1 from the RNAi-resistant transgene rescued the meiotic defects (four of four embryos; Supplemental Figure S2Ba). In contrast, mCherry::AIR-1^{K73RT201A} did not rescue the meiotic spindle defects (13 of 14 embryos), and the meiotic phenotype was equivalently severe in *air-1(RNAi)* embryos lacking or expressing AIR-1^{K73RT201A}, in that the MT spheres around chromosomes shrunk before establishing bipolarity (Figure 3A and Supplemental Figure S1B). Thus, in contrast to mitosis, the kinase activity of AIR-1 is required for the maintenance of MTs around chromosomes during meiotic prometaphase/metaphase.

AIR-1 is continuously required for the maintenance of MTs after bipolar spindle formation

After the establishment of bipolar spindle at meiotic prometaphase/metaphase, MTs are dynamically rearranged. In anaphase, concomitantly with the shortening of the bipolar spindle structure, interchromosomal MTs are formed between separating chromosomes. We next examined whether AIR-1 is involved in this process (Figure 3B). In the late meiotic anaphase of control embryos expressing GFP::β-tubulin and mCherry::Histone, interchromosomal MTs were detected between separating chromosome masses in all embryos (16 of 16), and some abnormalities were detected in 13% (two of 16) of them. On the other hand, after the disassembly of MT spheres in *air-1(RNAi)* meiotic embryos, chromosomes were not separated into two masses (11 of 12 embryos). In many cases (seven of 12), chromosomes stayed as a single mass, and MTs in their vicinity were not increased (Figure 3B). In some embryos (four of 12), chromosomes were partially separated into multiple masses, and MTs were detected between these separating chromosomes. Similarly, in embryos expressing a kinase-inactive form of AIR-1 (AIR-1^{K73RT201A}) in the absence of endogenous AIR-1, chromosomes stayed as a single mass without increasing the amount of MTs

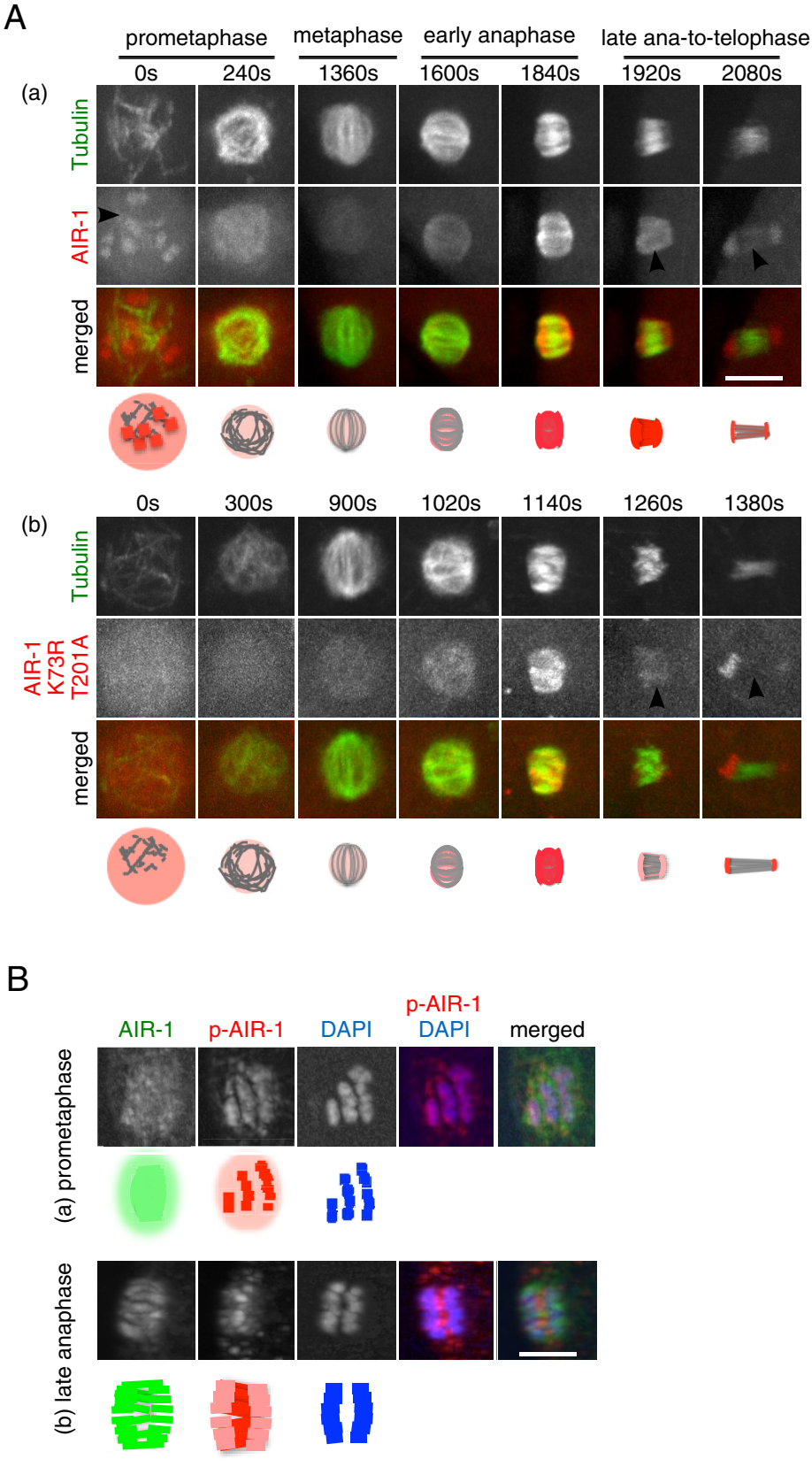

FIGURE 4: Localization of the kinase-active and the kinase-inactive forms of AIR-1 in meiotic embryos. (A) In utero time series images of meiotic embryos. (a) Embryo expressing mCherry::β-tubulin (green) and GFP::AIR-1 (red). (b) Embryo expressing GFP::β-tubulin (green) and mCherry::AIR-1^{K73RT201A} (kinase-inactive form; red). Frames were taken every 80 (a) or 60 (b) s, and representative images are shown. The time (in seconds) relative to GVBD is indicated. Bar, 5 μm. (B) Immunofluorescence images of female meiotic spindles stained with anti-AIR-1 antibody (green), anti-phospho-AIR-1 antibody, which recognizes the kinase-active form of AIR-1 (red), and DAPI (blue). (a) Prometaphase and (b) late anaphase. Bar, 5 μm.

around chromosomes (10 of 17 embryos; Figure 3B), or chromosomes were aberrantly separated, with morphologically abnormal interchromosomal MTs (six of 17 embryos). These phenotypes were not observed in embryos expressing wild-type AIR-1 from the RNAi-resistant transgene in the absence of endogenous AIR-1 (four of four; Supplemental Figure S2Bb). These results indicate that the AIR-1 kinase activity is required for meiotic anaphase and telophase.

To examine whether the late-anaphase defect of interchromosomal MT assembly is a secondary effect of MT destabilization during prometaphase/metaphase, we inhibited the AIR-1 kinase activity after the bipolarity of the spindle was established, using MLN8237, which inhibits the kinase activity of Aurora A preferentially to Aurora B (Manfredi *et al.*, 2011; Lioutas and Vernos, 2013). (In *C. elegans* mitotic embryos, 50 nM MLN8237 treatment phenocopied *air-1(RNAi)*, but inhibition of AIR-2/Aurora B was not detected; see *Materials and Methods* for details.) Meiotic embryos were treated with 50 nM MLN8237 after the assembly of bipolar spindles at early anaphase. Whereas the buffer-treated control embryos proceeded to telophase and formed interchromosomal MTs between separating chromosomes (four of four embryos; Figure 3Ca and Supplemental Video S2a), the MLN8237-treated embryos failed chromosome separation, and the amount of MTs remained low after the shrinkage of bipolar spindles (four of four embryos; Figure 3Cb and Supplemental Video S2b). These results suggest that the late anaphase defect caused by depletion of AIR-1 or inhibition of its kinase activity is not merely the secondary effect of the prometaphase defect, but it is required continuously throughout meiosis for the formation and/or maintenance of meiotic MTs.

AIR-1 kinase is locally activated within female meiotic spindles

To investigate at which sites the AIR-1 proteins works during female meiosis, we examined the localization of AIR-1 using the strain expressing GFP::AIR-1 (Figure 4A). In oocytes after GVBD, GFP::AIR-1 was detected as several objects in nuclei, likely

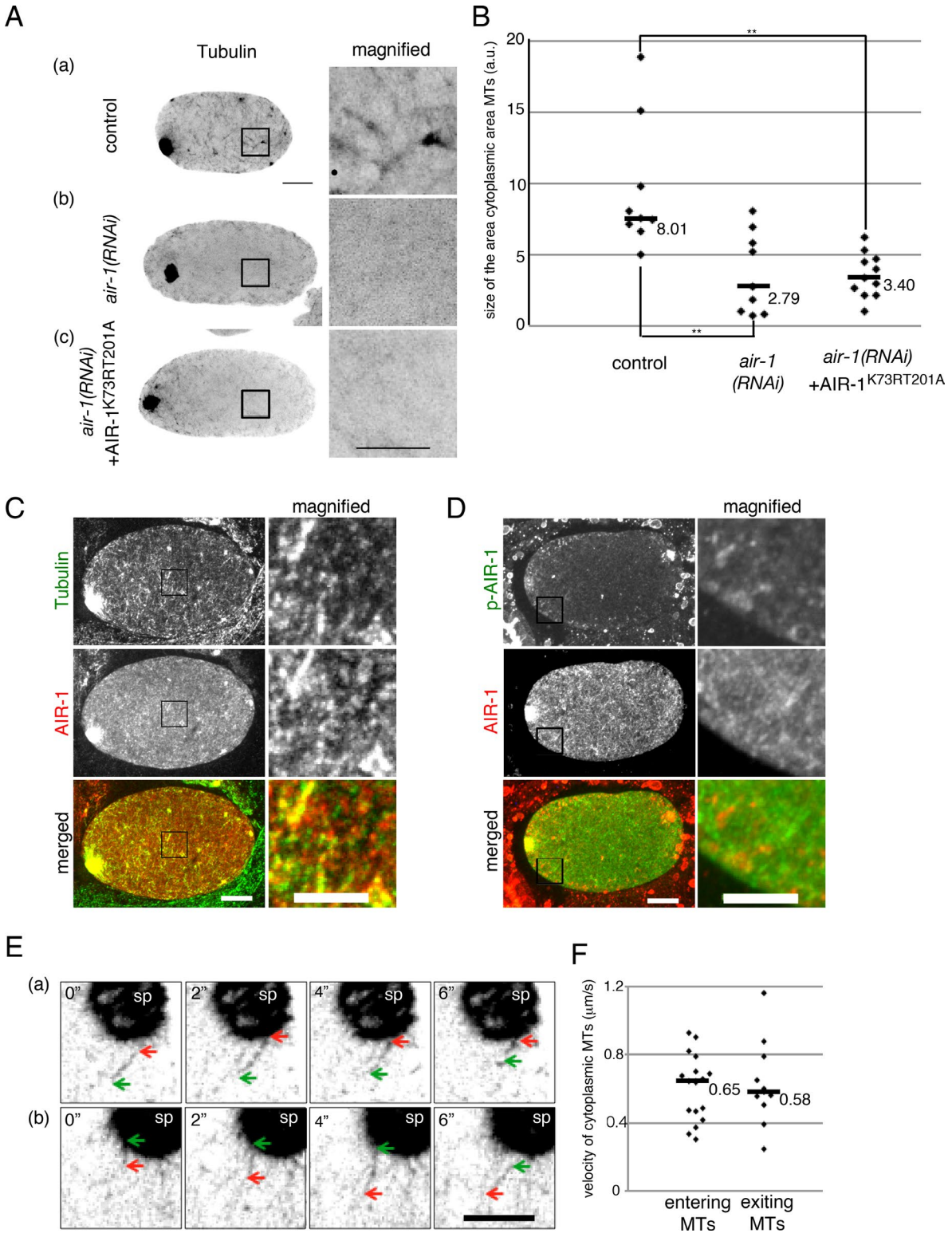

FIGURE 5: Kinase activity of AIR-1 is required for the formation and/or maintenance of cytoplasmic MTs in meiotic embryos. (A) Ex time-series images of meiotic embryos expressing GFP::β-tubulin (black). (a) Control embryo, (b) *air-1(RNAi)* embryo, and (c) *air-1(RNAi)* embryo expressing a kinase-inactive form of AIR-1 (AIR-1^{K73RT201A}). Right, magnified views. Bar, 10 μm (images showing whole embryos), 5 μm (magnified views). Contrast of original images was inverted and enhanced to visualize cytoplasmic MTs. (B) Quantification of cytoplasmic MTs in meiotic embryos. From images as shown in A, the size of the area covered with cytoplasmic MTs was measured and normalized by the size of the embryo. Each dot represents a single embryo (control, $n = 9$; *air-1(RNAi)*, $n = 9$; and *air-1(RNAi)*–expressing AIR-1^{K73RT201A}, $n = 11$). Pairs with significant difference, $^{**}p < 0.01$). (C) Localization of AIR-1 in the cytoplasm of a meiotic embryo at late anaphase. Immunofluorescence images of a meiotic embryo stained with an anti–α-tubulin antibody (green) and an anti–AIR-1 antibody (red) along with DAPI (blue). Right, magnified views of the cytoplasmic

corresponding to chromosomes (Figure 4Aa, 0 s, and Supplemental Video S3). At prometaphase, the GFP::AIR-1 signal was detected on MT spheres, which then diminished during metaphase (Figure 4Aa, 240, 1360 s). At anaphase, when the spindle was shortening, the GFP::AIR-1 signal on spindles was increased and enriched on spindle poles (Figure 4Aa, 1600, 1840 s). At late anaphase, GFP::AIR-1 was detected both on chromosomes and interchromosomal MTs at equivalent levels (Figure 4Aa, 1920 s). At telophase, as the interchromosomal MTs elongated, the GFP::AIR-1 signals on these MTs were diminished, whereas the chromosomal signal persisted (Figure 4Aa, 2080 s). Immunostaining with an anti–AIR-1 antibody that recognizes both the kinase-active and the kinase-inactive AIR-1 proteins (Toya *et al.*, 2011) showed consistent localization patterns with those with GFP::AIR-1 (Supplemental Figure S3).

Next, to examine when and where the kinase activity of AIR-1 is activated, we compared the foregoing AIR-1 localization patterns with those of the kinase-inactive form (Figure 4Ab and Supplemental Video S4) and the kinase-active form of AIR-1 (Figure 4B; under these experimental conditions, the endogenous AIR-1 was present). The localization of the kinase-inactive form of AIR-1 detected by mCherry::AIR-1^{K73RT201A} was similar to GFP::AIR-1, except for the following differences; mCherry::AIR-1^{K73RT201A} was not detected on chromosomes at GVBD (Figure 4Ab, 0 s), and its localization on interchromosomal MTs was weaker at late anaphase (Figure 4Ab, 1260 s) and absent at telophase (Figure 4Ab, 1380 s), whereas chromosomal signal persisted. The localization patterns of the kinase-active form of AIR-1 were examined by immunofluorescence with the anti–phospho-AIR-1 antibody (Toya *et al.*, 2011). The localization of the kinase-active form of AIR-1 was complementary to that of the kinase-inactive form; at prometaphase, the kinase-active form of AIR-1 enriched on and around chromosomes (Figure 4Ba); from metaphase to telophase, it was enriched in the areas where interchromosomal MTs were formed, but the signal on chromosomes was weaker (Figure 4Bb).

Collectively our data suggest that, whereas AIR-1 proteins are localized in the area where meiotic spindles are formed, their activation occurs at specific sites, especially on and around chromosomes during prometaphase and between chromosomes at late anaphase. These localization patterns are consistent with the phenotypes by depletion of the AIR-1 proteins or inhibition of the AIR-1 kinase activity.

The kinase activity of AIR-1 is required for the formation and/or maintenance of cytoplasmic MTs during female meiosis

In addition to the defects in meiotic spindle formation, we noticed that RNAi depletion of AIR-1 in meiotic embryos reduced cytoplasmic MTs. As described previously (Ellefson and McNally, 2009), in the control embryos at early anaphase, short, cytoplasmic MTs were present throughout the cytoplasm, with some enrichment at the cell cortex, where MT patches are often detected (Figure 5Aa). These cytoplasmic MTs gradually decreased during late anaphase. In *air-1(RNAi)* meiotic embryos, overall cytoplasmic MTs were reduced (Figure 5, Ab and B; area covered with cytoplasmic MTs was 35% [$n = 9$, $p < 0.01$] of that in the control [$n = 9$]). In embryos expressing the kinase-inactive AIR-1^{K73RT201A} in the *air-1(RNAi)* background, similar reduction of cytoplasmic MTs was observed (Figure 5, Ac and B; area covered with cytoplasmic MTs was reduced to 41% of the control [$n = 11$, $p < 0.01$]). Consistent with this, immunostaining revealed that AIR-1 partly colocalized with these cytoplasmic MTs (Figure 5C), and the kinase-active form of AIR-1 and short MTs were both enriched on the cell cortex (Figure 5D). These data imply that the kinase activity of AIR-1 is required for the formation and/or maintenance of cytoplasmic MTs during meiotic divisions, in addition to meiotic spindle MTs.

To investigate the interrelationship between the cytoplasmic MTs and the female meiotic spindle MTs, we analyzed the behavior of cytoplasmic MTs in meiotic embryos by live imaging. We found that the cytoplasmic MTs formed after GVBD dynamically moved within the cytoplasm, and a fraction of them entered (Figure 5Ea and Supplemental Video S5) and exited from (Figure 5Eb and Supplemental Video S6) the meiotic spindle. The MTs moved in either direction at nearly equivalent velocities (median velocity: entering MTs, 0.65 µm/s, $n = 17$; exiting MTs, 0.58 µm/s, $n = 11$, $p > 0.05$; Figure 5F). These observations raise the possibility that, in meiotic embryos, the short cytoplasmic MTs formed and/or maintained by AIR-1 may contribute to the formation of meiotic spindles.

In the mitosis of *C. elegans* early embryos, γ-tubulin–dependent MTs and AIR-1–dependent MTs coordinately assemble mitotic spindles (Toya *et al.*, 2011). Of note, for the assembly of mitotic AIR-1–dependent MTs, the kinase activity of AIR-1 is dispensable (Toya *et al.*, 2011). On the other hand, we found in this study that the kinase activity of AIR-1 is continuously required for the formation or the maintenance of meiotic MTs, including meiotic spindle MTs at prometaphase/metaphase, interchromosomal MTs at anaphase/telophase, and cytoplasmic MTs. Whether the kinase-inactive AIR-1 plays additional roles (as in mitotic cells) is unclear from this study. Our results also raise the possibility that a previously unknown, γ-tubulin– and AIR-1–independent MT assembly mechanism might contribute to the formation of meiotic spindle MTs before GVBD.

Aurora B, another Aurora kinase, is known to be required for multiple events during mitosis. Although the subcellular localizations of Aurora A and Aurora B are different, at least some of their functions and phosphorylation substrates appear to be shared (Hegarat *et al.*, 2011). For example, mammalian Aurora A and Aurora B both phosphorylates kinesin-13, which inactivates its MT-depolymerizing activity, thereby stabilizing MTs (Sampath *et al.*, 2004). In *C. elegans* meiosis, Aurora B/AIR-2 is required for the establishment of bipolarity of meiotic spindles and also likely for interchromosomal MT formation (Schumacher *et al.*, 1998b;

region. Contrast was enhanced to visualize cytoplasmic MTs. Bar, 10 µm. (D) Localization of the kinase-active form of AIR-1 in the cytoplasm of a meiotic embryo at late anaphase. Immunofluorescence images of a meiotic embryo stained with an anti–phospho-AIR-1 antibody (green), which recognizes the kinase-active form of AIR-1, and an anti–AIR-1 antibody (red), along with DAPI (blue). Right, magnified views. Contrast was enhanced to visualize cytoplasmic MTs. Bar, 10 µm. (E) Movement of cytoplasmic MTs in meiotic embryos. Ex vivo time-series images of cytoplasmic MTs around a meiotic spindle visualized with GFP::β-tubulin. Green and red arrows indicate two ends of moving cytoplasmic MTs. (a) MT entering the meiotic spindle. (b) MT exiting the meiotic spindle. Frames were taken every 2 s. Indicated is the time (in seconds) elapsed from the start of the movie. Contrast was inverted and enhanced to visualize cytoplasmic MTs. sp, meiotic spindle. Bar, 5 µm. (F) Velocity of cytoplasmic MTs. Each dot represents the velocity of cytoplasmic MTs entering or exiting meiotic spindles. Data were collected from four meiotic embryos.

Dumont *et al.*, 2010). A requirement of both AIR-1 and AIR-2 in meiotic spindle formation implies some coordinated roles of these two related kinases. We speculate that AIR-1 and AIR-2 might phosphorylate kinesin-13 (*C. elegans* KLP-7) to inactivate its MT-depolymerizing activity during *C. elegans* meiosis, which may contribute to the stabilization of spindle and interchromosomal MTs. Further work is necessary to unravel the coordinated roles of these Aurora kinases during meiosis.

MATERIALS AND METHODS

Strains and culture

C. elegans strains were derived from the wild-type Bristol strain N2 and cultured as described (Brenner, 1974). The following strains were used in this study. Wild-type strain N2, SA250 (*tjIs54[pie-1promoter-gfp::tbb-2; pie-1promoter-2xmCherry::tbg-1; unc-119+]; tjIs57[pie-1 promoter-mCherry::H2B (his-48); unc-119+]*), SA378 (*unc-119(ed3)III;tjIs173[pie-1_promoter_1xgfp::air-1r unc-119(+)]*), and SA511 (*unc-119(ed3)III;tjIs257[pie-1promoter-mCherry::air-1r K73R T201A unc-119(+)];ruIs48[unc-119(+) pie-1::tubulin::GFP fusion]*; source for the foregoing three strains, Toya *et al.*, 2011), SA729 (*unc-119(ed3) III;tjIs57;tjIs257;ruIs48*), SA772 (*unc-119(ed3) III;tjIs332[pie-1promoter::mCherry::TBB-2+ unc-119(+)]*), SA796 *(unc-119(ed3)III;tjIs173;tjIs332)*, SA855 (*tjTi1[pie-1p:gfp:aspm-1;neoR] V*), and SA860 (*unc-119(ed3)III;tjIs332;tjTi1 V*). SA772 was made by ballistic transformation (Praitis *et al.*, 2001). SA855 was made by the miniMos technique (Frokjaer-Jensen *et al.*, 2014) using a NeoR plasmid carrying the *pie-1* promoter-driven genomic *aspm-1* fragment with the *gfp* coding sequence at the 5′ of *aspm-1* open reading frame. All strains were maintained at 24.5°C.

To evaluate the amount of GFP/mCherry-tagged AIR-1 protein derived from RNAi-resistant transgenes in SA378 (GFP::AIR-1) and SA511 (mCherry::AIR-1^{K73RT201A}) versus endogenous AIR-1, we performed Western blotting using anti-AIR-1 antibodies against the lysates of gravid adults. To estimate the amount of AIR-1 and its derivatives, we measured the intensities of the chemical luminescence of the bands corresponding to each protein on the Western blot membrane using ImageJ software (National Institutes of Health, Bethesda, MD).

RNAi

RNAi was carried out by the soaking method as described (Maeda *et al.*, 2001). cDNA clones used to synthesize double-stranded RNA (dsRNA) were as follows: yk364b4 for full-length *air-1* and yk1562g08 for *tbg-1* (gifts from Y. Kohara, National Institute of Genetics, Mishima, Japan), pNKair-1N (Toya *et al.*, 2011) for *air-1N(RNAi)*, and pENTERNdeIair1r cDNA (Toya *et al.*, 2011) for *air-1R(RNAi)*. *air-1N(RNAi)* was used to deplete the endogenous AIR-1 without affecting the transcript of the RNAi-resistant *air-1* transgene (*air-1R*). *air-1R(RNAi)* was used to deplete the transcript of the *air-1R* transgene. Worms were soaked in dsRNA solution at concentrations of 2 mg/ml for each dsRNA species, incubated at 24.5°C, and removed from the dsRNA solution to seeded nematode growth media plates. Worms were then cultured at 24.5°C and observed. Soaking period and observation time after the recovery from dsRNA solution were as follows: full-length *air-1(RNAi)*, 24 and 22 h; *air-1N(RNAi)*, 24 and 22 h; and *tbg-1(RNAi)*, 37 and 16 h. For *air-1N(RNAi);air-1R(RNAi)*, worms were soaked in *air-1R* dsRNA solution for 6 h, and then *air-1N* dsRNA was added and incubated for an additional 24 h; worms were observed later than 22 h after the recovery. For *air-1(RNAi);tbg-1(RNAi)*, worms were soaked in the *tbg-1* dsRNA solution for 24 h, and then *air-1* dsRNA was added and incubated for an additional 14 h; worms were observed >22 h after the recovery. The efficiencies of TBG-1 depletion by RNAi were confirmed by the absence of mCherry::TBG-1 signal on centrosomes in mitotic embryos (Supplemental Figure S1).

Microscopy

For time-lapse microscopy, the specimens were imaged with a CSU-X1 spinning-disk confocal system (Yokogawa Electric, Musashino, Japan) mounted on an IX71 inverted microscope (Olympus, Tokyo, Japan) controlled by MetaMorph software (Molecular Devices, Sunnyvale, CA). Images were acquired every 30–80 s with an Orca-R2 12-bit/16-bit cooled charge-coupled device camera (Hamamatsu Photonics, Hamamatsu, Japan) and a 60×/1.30 numerical aperture silicone objective lens (Olympus) without binning with streaming. To obtain *Z*-sectioned images of meiotic spindles, 7–25 *Z*-sections at 1-μm steps were acquired using 300- to 500-ms exposures with 255 camera gain parameter for each wavelength. To quantify fluorescence intensities, 28 *Z*-sections with 0.5-μm steps were acquired using 500-ms exposures with 255 camera gain parameter for each wavelength, with 60-s time intervals. For the analysis of the cytoplasmic MT behavior, single–focal plane images of SA250 meiotic embryo under ex vivo conditions were acquired using 1200-ms exposures with 50 camera gain parameter for GFP::β-tubulin and 150-ms exposures with 255 camera gain parameter for mCherry::Histone, with 2-s intervals. Captured images were processed and analyzed with ImageJ and processed with Inkscape software (The Inkscape Team, https://inkscape.org/) and Adobe Illustrator CS6 for presentation. Single–time point images were obtained and analyzed with basically the same procedure as that for time-lapse images.

Observation of meiosis

For in utero live imaging of meiotic embryos, gravid adult worms expressing fluorescently tagged proteins were anesthetized with 1 mM levamisole in egg buffer (Edgar, 1995) and mounted on 2% agarose pads. The ex vivo live imaging of meiotic embryos was carried out as described (Dumont *et al.*, 2010), with the following modifications. Instead of the 24 mm × 60 mm coverslip with a metal holder, a slide glass (Matsunami, Kishiwada, Japan) with a circle drawn by PAP-Pen (Daido Sangyo, Toda, Japan) was used. Vaseline was used as a spacer between the coverslip and the slide glass.

For immunofluorescence microscopy, embryos were fixed and stained using rat anti–AIR-1 (1:50; Toya *et al.*, 2011), rabbit anti-p-AIR-1 (Toya *et al.*, 2011), and mouse monoclonal anti–α-tubulin (1:500; DM1A; Sigma-Aldrich, St. Louis, MO) as described previously (Toya *et al.*, 2011). The secondary antibodies used were Alexa 488–conjugated goat anti-rabbit immunoglobulin G (IgG; 1:1000; Thermo Fisher Scientific, Waltham, MA), Alexa 568–conjugated goat anti-rabbit IgG (1:1000; Thermo Fisher Scientific), and Alexa 568–conjugated goat anti-rat IgG (1:1000; Thermo Fisher Scientific). DNA was counterstained with the 4,6-diamidino-2-phenylindole (DAPI)–containing mounting solution Vectashield (Vector Laboratories, Burlingame, CA). Images were acquired with the same setting for the time-lapse microscopy. Images of 10–26 serial *z*-axis sections with a 1–μm step size were taken. RNAi depletion of AIR-1 greatly diminished the staining, indicating that this staining in meiotic embryos reflected the localization of the endogenous AIR-1.

MLN8237 treatment of meiotic embryos

To inhibit the kinase activity of AIR-1, we used an Aurora kinase inhibitor, MLN8237 (Manfredi *et al.*, 2011; Lioutas and Vernos, 2013). We confirmed that, in *C. elegans*, 50 nM MLN8237 preferentially inhibited AIR-1 kinase but not AIR-2/Aurora B, by treating mitotic

embryos; under this condition, it caused phenotypes characteristic of AIR-1 depletion, such as defects of centrosome maturation, pronuclear migration, and spindle formation (four of four embryos), without causing phenotypes characteristic of AIR-2/Aurora B depletion, such as chromosome condensation defect (zero of four embryos). For AIR-1 inhibition during female meiotic metaphase to early anaphase, 50 nM MLN8237 treatment was carried out ex vivo because meiotic embryos before eggshell formation are permeable to MLN8237. Meiotic embryos were dissected in a drop of 2 µl of meiosis buffer containing 1% dimethyl sulfoxide (DMSO) and observed. As the first time point, images of meiotic spindles before drug treatment were taken. Then 2 µl of meiosis buffer with 1% DMSO and 100 nM MLN8237 (final concentration 50 nM) was added between the coverslip and the slide glass with a micropipette, and meiosis was recorded.

Image processing and analysis

To estimate the amount of MT in the meiotic spindle, the total fluorescent intensity of GFP::β-tubulin in the spindle region of each *Z*-plane in the *Z*-sectioned image stacks at 120 and 720 s after GVBD was measured using ImageJ and normalized by the total fluorescence intensity of mCherry::Histone in the spindle region as measured by the same manner as GFP::β-tubulin.

To visualize the behavior of cytoplasmic MTs, *Z*-sectioned image stacks were projected using the maximum intensity algorithm of ImageJ. Images were processed with a median filter for each image using the "median" algorithm with seven pixels, and the intensity of each pixel was reduced to 50% using the "divide" algorithm. The resulting filter was subtracted from the original images to generate the processed image. The color of the resulting image was inverted with the Edit LUT command.

To measure the velocity of cytoplasmic MTs moving in and out of meiotic spindles, the position of the leading end of moving MTs was manually tracked and the length of their trajectories was measured. The velocity of each MT movement was calculated with the length of the trajectory and the time elapsed during the movement. The velocity of 17 MTs entering the spindle and 11 MTs exiting the spindle was measured in four independent meiotic embryos.

For anti-AIR-1 and anti-p-AIR-1 staining in Figure 4B, *Z*-sectioned images were processed with the median filter as described and three dimensionally reconstructed using the volume viewer plug-in in ImageJ.

To estimate the area of cytoplasm covered with cytoplasmic MTs, 160 × 160–pixel rectangular regions of interest in the cytoplasm in *Z*-projected images were filtered by the Threshold function of ImageJ with the Yen algorithm to detect the area with cytoplasmic MTs.

Statistical analysis

Statistical analysis was performed with Microsoft Excel software or MEPHAS (www.gen-info.osaka-u.ac.jp/testdocs/tomocom/). A Mann–Whitney *U* test was used to compare nonpaired data sets. Fischer's exact test was used to compare frequencies of phenotypes.

ACKNOWLEDGMENTS

We thank the *Caenorhabditis* Genetics Center (funded by the National Institutes of Health Center for Research Resources) for providing strains, Yuji Kohara (National Institutes of Genetics, Mishima, Japan) for providing cDNA clones, and Sugimoto lab members for useful discussions. This work was supported by NEXT Program LS006 from the Cabinet Office, Government of Japan, and grants from the Takeda Science Foundation, the Novartis Foundation, and the Mitsubishi Foundation to A.S.

REFFERENCES

Albertson DG, Thomson JN (1993). Segregation of holocentric chromosomes at meiosis in the nematode, Caenorhabditis elegans. Chromosome Res 1, 15–26.

Barrett SL, Albertini DF (2007). Allocation of gamma-tubulin between oocyte cortex and meiotic spindle influences asymmetric cytokinesis in the mouse oocyte. Biol Reprod 76, 949–957.

Barros TP, Kinoshita K, Hyman AA, Raff JW (2005). Aurora A activates D-TACC-Msps complexes exclusively at centrosomes to stabilize centrosomal microtubules. J Cell Biol 170, 1039–1046.

Bobinnec Y, Fukuda M, Nishida E (2000). Identification and characterization of Caenorhabditis elegans gamma-tubulin in dividing cells and differentiated tissues. J Cell Sci 113, 3747–3759.

Brenner S (1974). The genetics of Caenorhabditis elegans. Genetics 77, 71–94.

Carazo-Salas RE, Guarguaglini G, Gruss OJ, Segref A, Karsenti E, Mattaj IW (1999). Generation of GTP-bound Ran by RCC1 is required for chromatin-induced mitotic spindle formation. Nature 400, 178–181.

Connolly AA, Osterberg V, Christensen S, Price M, Lu C, Chicas-Cruz K, Lockery S, Mains PE, Bowerman B (2014). Caenorhabditis elegans oocyte meiotic spindle pole assembly requires microtubule severing and the calponin homology domain protein ASPM-1. Mol Biol Cell 25, 1298–1311.

Ding J, Swain JE, Smith GD (2011). Aurora kinase-A regulates microtubule organizing center (MTOC) localization, chromosome dynamics, and histone-H3 phosphorylation in mouse oocytes. Mol Reprod Dev 78, 80–90.

Dumont J, Oegema K, Desai A (2010). A kinetochore-independent mechanism drives anaphase chromosome separation during acentrosomal meiosis. Nat Cell Biol 12, 894–901.

Dumont J, Petri S, Pellegrin F, Terret ME, Bohnsack MT, Rassinier P, Georget V, Kalab P, Gruss OJ, Verlhac MH (2007). A centriole- and RanGTP-independent spindle assembly pathway in meiosis I of vertebrate oocytes. J Cell Biol 176, 295–305.

Edgar LG (1995). Blastomere culture and analysis. Methods Cell Biol 48, 303–321.

Ellefson ML, McNally FJ (2009). Kinesin-1 and cytoplasmic dynein act sequentially to move the meiotic spindle to the oocyte cortex in Caenorhabditis elegans. Mol Biol Cell 20, 2722–2730.

Frokjaer-Jensen C, Davis MW, Sarov M, Taylor J, Flibotte S, LaBella M, Pozniakovsky A, Moerman DG, Jorgensen EM (2014). Random and targeted transgene insertion in Caenorhabditis elegans using a modified Mos1 transposon. Nat Methods 11, 529–534.

Gard DL (1992). Microtubule organization during maturation of Xenopus oocytes: assembly and rotation of the meiotic spindles. Dev Biol 151, 516–530.

Glover DM, Leibowitz MH, McLean DA, Parry H (1995). Mutations in aurora prevent centrosome separation leading to the formation of monopolar spindles. Cell 81, 95–105.

Gruss OJ, Carazo-Salas RE, Schatz CA, Guarguaglini G, Kast J, Wilm M, Le Bot N, Vernos I, Karsenti E, Mattaj IW (2001). Ran induces spindle assembly by reversing the inhibitory effect of importin alpha on TPX2 activity. Cell 104, 83–93.

Hannak E, Kirkham M, Hyman AA, Oegema K (2001). Aurora-A kinase is required for centrosome maturation in Caenorhabditis elegans. J Cell Biol 155, 1109–1116.

Heald R, Tournebize R, Blank T, Sandaltzopoulos R, Becker P, Hyman A, Karsenti E (1996). Self-organization of microtubules into bipolar spindles around artificial chromosomes in Xenopus egg extracts. Nature 382, 420–425.

Hegarat N, Smith E, Nayak G, Takeda S, Eyers PA, Hochegger H (2011). Aurora A and Aurora B jointly coordinate chromosome segregation and anaphase microtubule dynamics. J Cell Biol 195, 1103–1113.

Khodjakov A, Cole RW, Oakley BR, Rieder CL (2000). Centrosome-independent mitotic spindle formation in vertebrates. Curr Biol 10, 59–67.

Lioutas A, Vernos I (2013). Aurora A kinase and its substrate TACC3 are required for central spindle assembly. EMBO Rep 14, 829–836.

Ma W, Baumann C, Viveiros MM (2010). NEDD1 is crucial for meiotic spindle stability and accurate chromosome segregation in mammalian oocytes. Dev Biol 339, 439–450.

Maeda I, Kohara Y, Yamamoto M, Sugimoto A (2001). Large-scale analysis of gene function in Caenorhabditis elegans by high-throughput RNAi. Curr Biol 11, 171–176.

Manfredi MG, Ecsedy JA, Chakravarty A, Silverman L, Zhang M, Hoar KM, Stroud SG, Chen W, Shinde V, Huck JJ, *et al.* (2011). Characterization of Alisertib (MLN8237), an investigational small-molecule inhibitor

of aurora A kinase using novel in vivo pharmacodynamic assays. Clin Cancer Res 17, 7614–7624.
McNally K, Audhya A, Oegema K, McNally FJ (2006). Katanin controls mitotic and meiotic spindle length. J Cell Biol 175, 881–891.
Motegi F, Velarde NV, Piano F, Sugimoto A (2006). Two phases of astral microtubule activity during cytokinesis in C. elegans embryos. Dev Cell 10, 509–520.
Nachury MV, Maresca TJ, Salmon WC, Waterman-Storer CM, Heald R, Weis K (2001). Importin beta is a mitotic target of the small GTPase Ran in spindle assembly. Cell 104, 95–106.
Praitis V, Casey E, Collar D, Austin J (2001). Creation of low-copy integrated transgenic lines in Caenorhabditis elegans. Genetics 157, 1217–1226.
Reboutier D, Troadec MB, Cremet JY, Chauvin L, Guen V, Salaun P, Prigent C (2013). Aurora A is involved in central spindle assembly through phosphorylation of Ser 19 in P150Glued. J Cell Biol 201, 65–79.
Riparbelli MG, Callaini G, Glover DM, Avides Mdo C (2002). A requirement for the Abnormal Spindle protein to organise microtubules of the central spindle for cytokinesis in Drosophila. J Cell Sci 115, 913–922.
Sampath SC, Ohi R, Leismann O, Salic A, Pozniakovski A, Funabiki H (2004). The chromosomal passenger complex is required for chromatin-induced microtubule stabilization and spindle assembly. Cell 118, 187–202.
Sawada T, Schatten G (1988). Microtubules in ascidian eggs during meiosis, fertilization, and mitosis. Cell Motil Cytoskeleton 9, 219–230.
Schatten G (1994). The centrosome and its mode of inheritance: the reduction of the centrosome during gametogenesis and its restoration during fertilization. Dev Biol 165, 299–335.
Schuh M, Ellenberg J (2007). Self-organization of MTOCs replaces centrosome function during acentrosomal spindle assembly in live mouse oocytes. Cell 130, 484–498.
Schumacher JM, Ashcroft N, Donovan PJ, Golden A (1998a). A highly conserved centrosomal kinase, AIR-1, is required for accurate cell cycle progression and segregation of developmental factors in Caenorhabditis elegans embryos. Development 125, 4391–4402.
Schumacher JM, Golden A, Donovan PJ (1998b). AIR-2: an Aurora/Ipl1-related protein kinase associated with chromosomes and midbody microtubules is required for polar body extrusion and cytokinesis in Caenorhabditis elegans embryos. J Cell Biol 143, 1635–1646.
Tavosanis G, Llamazares S, Goulielmos G, Gonzalez C (1997). Essential role for gamma-tubulin in the acentriolar female meiotic spindle of Drosophila. EMBO J 16, 1809–1819.
Toya M, Terasawa M, Nagata K, Iida Y, Sugimoto A (2011). A kinase-independent role for Aurora A in the assembly of mitotic spindle microtubules in Caenorhabditis elegans embryos. Nat Cell Biol 13, 708–714.
Tsai MY, Zheng Y (2005). Aurora A kinase-coated beads function as microtubule-organizing centers and enhance RanGTP-induced spindle assembly. Curr Biol 15, 2156–2163.
van der Voet M, Lorson MA, Srinivasan DG, Bennett KL, van den Heuvel S (2009). C. elegans mitotic cyclins have distinct as well as overlapping functions in chromosome segregation. Cell Cycle 8, 4091–4102.
Yang HY, McNally K, McNally FJ (2003). MEI-1/katanin is required for translocation of the meiosis I spindle to the oocyte cortex in C elegans. Dev Biol 260, 245–259.